



Published in final edited form as:

*Mol Genet Metab.* 2017 June ; 121(2): 150–156. doi:10.1016/j.ymgme.2017.04.008.

## Crystal structure of a mutant glycosylasparaginase shedding light on aspartylglycosaminurea-causing mechanism as well as on hydrolysis of non-chitobiose substrate

Suchita Pande<sup>1</sup>, Damodharan Lakshminarasimhan<sup>2</sup>, and Hwai-Chen Guo<sup>3</sup>

<sup>1</sup>Department of Biological Sciences, University of Massachusetts Lowell, 1 University Avenue, Lowell, MA 01854, USA

<sup>2</sup>Department of Biological Sciences, University of Massachusetts Lowell, 1 University Avenue, Lowell, MA 01854, USA; Current Address: Xtal Biostructures Inc, 12 Michigan Drive, Natick, MA 01760, USA

<sup>3</sup>Department of Biological Sciences, University of Massachusetts Lowell, 1 University Avenue, Lowell, MA 01854, USA

### Abstract

Glycosylasparaginase (GA) is an amidase that cleaves Asn-linked glycoproteins in lysosomes. Deficiency of this enzyme causes accumulation of glycoasparagines in lysosomes of cells, resulting in a genetic condition called aspartylglycosaminuria (AGU). To better understand the mechanism of a disease-causing mutation with a single residue change from a glycine to an aspartic acid, we generated a model mutant enzyme at the corresponding position (named G172D mutant). Here we report a 1.8Å resolution crystal structure of mature G172D mutant and analyzed the reason behind its low hydrolase activity. Comparison of mature G172D and wildtype GA models reveals that the presence of Asp 172 near the catalytic site affects substrate catabolism in mature G172D, making it less efficient in substrate processing. Also recent studies suggest that GA is capable of processing substrates that lack a chitobiose (Glycan, N-acetylchitobios, NAcGlc) moiety, by its exo-hydrolase activity. The mechanism for this type of catalysis is not yet clear. L-aspartic acid  $\beta$ -hydroxamate ( $\beta$ -AHA) is a non-chitobiose substrate that is known to interact with GA. To study the underlying mechanism of non-chitobiose substrate processing, we built a GA- $\beta$ -AHA complex structure by comparing to a previously published G172D mutant precursor in complex with a  $\beta$ -AHA molecule. A hydrolysis mechanism of  $\beta$ -AHA by GA is proposed based on this complex model.

### Keywords

Glycosylasparaginase; Aspartylglycosaminuria;  $\beta$ -AHA; catalytic mechanism

---

**Publisher's Disclaimer:** This is a PDF file of an unedited manuscript that has been accepted for publication. As a service to our customers we are providing this early version of the manuscript. The manuscript will undergo copyediting, typesetting, and review of the resulting proof before it is published in its final citable form. Please note that during the production process errors may be discovered which could affect the content, and all legal disclaimers that apply to the journal pertain.

### Conflict of Interest

The authors declare no conflict of interest.

## 1. Introduction

Glycosylasparaginase (GA) belongs to the family of N-terminal nucleophile (Ntn) hydrolases that can hydrolyze various compounds carrying L-asparagine residue with free  $\alpha$ -amino and  $\alpha$ -carboxylate groups [1, 2]. It is a lysosomal amidase which processes L-asparagine linked glycoproteins into smaller units of free amino acids and sugars essential for several metabolic pathways of the body [2, 3]. GA is initially synthesized as an inactive single-polypeptide precursor in which  $\alpha$  and  $\beta$ -subunits are joined together via a surface loop (called precursor- or P-loop) that blocks the catalytic center of this enzyme [4, 5]. A consequent autoproteolysis results in a main-chain cleavage at the P-loop by a self-catalyzed peptide bond rearrangement through an N $\rightarrow$ O acyl shift, and results in an active form of the hydrolase with  $\alpha$  and  $\beta$ -subunits [5–7]. The N-terminal  $\gamma$ -hydroxyl and  $\alpha$ -amino group of threonine residue of the newly formed  $\beta$ -subunit acts as an active site nucleophile and the general base, respectively, in the hydrolysis of N-glycosidic bonds of Asn-linked glycoproteins [6–8].

Autoproteolysis of GA precursor could be impaired by a missense mutation. Such a mutation results in a lysosomal storage disease called aspartylglucosaminuria (AGU) which occurs due to misprocessing of asparagine linked glycoproteins. This leads to accumulation of aspartylglucosamine (NAcGlc-Asn) and other glycoconjugates of aspartylglucosamine moiety at the reducing end in body fluids and tissues [9–11]. AGU results in progressive impairment of brain, motor and skeletal development of the patients [11, 12].

Catalytic activity of GA is not just restricted to a few substrates but is known to be involved in hydrolysis of various Asn-linked glycoprotein substrates and L-asparagine analogues (Fig. 1). GA is capable of hydrolyzing L-asparagine via  $\beta$ -aspartyl intermediate to form L-aspartic acid and ammonia [13]. It is also known to be involved in the metabolism of  $\beta$  aspartyl peptides. It hydrolyzes  $\beta$ -aspartyl peptides to form L-aspartic acid and other peptides and synthesize  $\beta$ -aspartyl peptides from  $\beta$ -aspartylglycosylamine. GA utilizes L-asparagine as  $\beta$ -aspartyl donor towards the formation of  $\beta$ -aspartyl peptides [14].  $\beta$ -aspartyl enzyme formation occurs after elimination of ammonia during the hydrolysis of L-asparagines by GA [13]. Studies suggest that L-aspartic acid  $\beta$ -hydroxamate ( $\beta$ -AHA) and L-aspartic acid beta methyl ester can also be hydrolyzed by GA even though these substrates lack the di N-acetylchitobios (chitobiose, NAcGlc-NAcGlc) moiety [15]. These results underline that GA shows exo-type hydrolase activity with various glycoasparagines and its reaction mechanism requires a  $\beta$ -aspartyl enzyme intermediate [15]. However a detailed reaction mechanism behind the catalysis of such non-chitobiose substrate remains unclear.

In an AGU allele of a Canadian family, a mutation has been reported that is caused by the change of a nucleotide from G to A in exon 6 [16, 17], causing complex clinical presentation [18]. This mutation leads to two alternative splicing forms, resulting in two different lengths of transcripts: one with the normal length, whereas the other with a truncation of about 90 nucleotides due to exon 6 skipping. The truncated transcript is labile and likely to encode a misfolded protein due to a translational frameshift. On the other hand, the normal length transcript translates into a missense mutant that changes residue 203 of human GA from a

glycine to an aspartic acid [16]. To study the disease-causing mechanism of this missense mutant, we report here a 1.8Å resolution structure of a model missense GA corresponding to this Canadian AGU allele. We also propose a plausible explanation for its low activity based on comparison of substrate bound complexes of the mutant model with the wildtype GA model. Since a precursor structure of the same mutant in complex with  $\beta$ -AHA has also been reported previously [17], in this study we further built a GA- $\beta$ -AHA model complex by superposing a few GA structures: the current model, the precursor- $\beta$ -AHA complex, and the wild-type GA structures [7, 17]. This allows us to analyze catalysis of  $\beta$ -AHA as a non-chitobiose substrate of GA.

## 2. Material and Methods

### 2.1. Enzyme Activity Assay

Aspartic acid  $\beta$ -(p-nitroanilide) (Asp(pNA)-OH) was used as a substrate analog for this assay, which forms p-nitroaniline after hydrolysis reaction by glycosylasparaginase (GA). Each reaction was in a volume of 100 $\mu$ l of 50mM Tris buffer, pH 7.5, containing appropriate concentration of aspartic acid  $\beta$ -(p-nitroanilide). To monitor enzyme activity, substrate was incubated for 1hr at 37°C and release of p-nitroaniline is monitored at 405nm using Spectramax-M2 spectrophotometer.

### 2.2. Crystallization

GA mutant protein were over-expressed, purified by the published protocol of GA Flavobacterium [19]. Protein crystallizations was undertaken with Hampton Research Index crystal screen conditions. The mature form G172D crystals were obtained in 0.2M Ammonium Acetate, 0.1M Bis-Tris pH 5.5, 25% polyethylene glycol 3350 after removal of glycine through 10kDa cutoff amicon centrifugal filter.

### 2.3. Data Collection and processing

For data collection, crystals were cryoprotected in reservoir solution with 20% glycerol. X-ray data were collected using the beamline X29 at National Synchrotron Light Source at Brookhaven. The data were processed with the iMosflm and scaled and merged using Aimless program in CCP4 suite [20]. The space group of the crystal was P1 with two protein molecules in an asymmetric unit.

### 2.4. Structural Refinement

The crystal structure of G172D mutant was solved by molecular replacement method, using the previously published GA D151N mutant protein structure (PDB code 1P4K) [21] as search model. Molecular replacement (MR) was performed with Molrep. Refinement was done using Refmac program by excluding 5% of the total reflection data from the refinement cycles and used to calculate the free R factor ( $R_{free}$ ) for monitoring refinement progress. This MR model was further refined by rigid body and restrained refinements. Model building was carried out using COOT [22] to obtain the final structure. In the Ramachandran plot, all residues except one (0.4%) of the model are located in the most favorable or allowed regions. The outlier residue is Trp 11 in each molecule of this structure. Several attempts to modify this outlier to a favorable geometry always returned to its original geometry after

refinement. Trp 11 is an active site residue the current model fits well into the electron density map. Thus the unusual configuration of Trp 11 appears to be valid and stabilized through interactions with nearby active site residues. Detailed statistics of X-ray data collection, processing, and structure refinement statistics are summarized in Table 1. Structural presentations were prepared using PyMOL (Delano Scientific) and Chemdoodle (iChemLabs).

## 2.5. Structural comparisons

Structural superimpositions of different structures were done using Superpose from the CCP4 suite [20]. RMSDs of all the main chain atoms of equivalent residues were calculated for comparisons.

## 2.6. Model building

The  $\beta$ -AHA-GA complex model was generated by superimposing secondary structure of G172D- $\beta$ -AHA complex (precursor structure, PDB code 4R4Y) [17] with the previously published T152C GA-NAcGlc-Asn complex (GA-substrate structure, PDB code 2GL9) [23]. The coordinates of the  $\beta$ -AHA were then placed in the active site of the wild-type GA structure, built as described previously (2GAW) [7].

G172D-NAcGlc-Asn complex was generated by superimposing secondary structure of G172D mature structure with the previously published T152C GA-NAcGlc-Asn complex (GA-substrate structure, PDB code 2GL9) [23]. The coordinates of the NAcGlc-Asn substrate were then placed into the current apo-G172D structure.

## 2.7. Accession Numbers

The atomic coordinates and structure factors have been deposited in the Protein Data Bank with ID code 5V2I.

## 3. Results

### 3.1. Relative Hydrolase Activity of G172D mutant

To study effects of point mutation on GA structure, we generated an AGU model enzyme equivalent to the Canadian allele in which a point mutation of nucleotide G to A changes residue 203 from glycine to aspartic acid in humans [16, 17]. Due to the difficulty in expressing and purifying human GA protein [24], *Flavobacterium* homolog was used as a model enzyme. This is feasible because amino acid sequences of human and *Flavobacterium* GAs are significantly homologous and have a conserved  $\alpha\beta\beta\alpha$  fold with an identical autoproteolytic center [7,8]. Therefore, a Gly-to-Asp AGU mutation at the equivalent position of *Flavobacterium* GA, at residue 172 (named G172D mutant), was generated as a model enzyme of the Canadian mutation to study the effect of the disease-causing mechanism.

Purified G172D mutant was compared to the wild type GA to examine its autoproteolytic and hydrolytic activities. Unlike wild type GA precursor which autoproteolyzes spontaneously into the functional mature form with  $\alpha$  and  $\beta$  subunits, G172D mutant

retained as a single-chain precursor after a 2-days' purification procedure (Fig. 2A). The downstream hydrolytic activities of wild type GA and G172D were further examined using a substrate analog of GA, aspartic acid  $\beta$ -(p-nitroanilide). Compared to the wild type GA, G172D had insignificant amount of hydrolase activity (1.2%) which is consistent with the gel analysis that G172D was purified in its precursor form and therefore retained as an inactive precursor (Fig. 2B).

### 3.2. Structure of G172D mature form mutant

We previously reported a precursor structure of the G172D mutant in the presence of autoproteolysis inhibitor [17]. It is evident from our previous studies that the G172D precursor protein can autoproteolyze to mature form during several days of crystallization process [17]. In this report, we have prepared a new crystal form in the absence of autoproteolysis inhibitor to study structures of autoproteolyzed G172D mutant. Even though precursor G172D protein was initially used to setup crystals, electron density map clearly indicate that the P-loop (residues 137-151) linking  $\alpha$  and  $\beta$  subunits in the precursor had been broken in both molecules of the asymmetric unit. The space group and cell constants of current G172D mature form crystal (P1,  $a = 46.0$ ,  $b = 52.8$ ,  $c = 61.9$  Å;  $\alpha = 81.5$ ,  $\beta = 90.2$ ,  $\gamma = 105.9^\circ$ ) are very similar to previously published precursor form crystals (PDB code 9GAC and 9GAF) [4, 19]. The fact that the space group of the new crystal form is the same as other GA precursors, but is different from other mature enzymes [7, 19, 23], suggests that in this study the G172D mutant was initially packed into the crystal as a precursor, then slowly got autocleaved into mature form inside current crystal form. Previously we demonstrated that GA dimerization is essential to trigger autoproteolysis [25]. It now appears that crystallization/oligomerization could have also facilitated the autoprocessing of the G172D precursor. With the new crystal form, crystal structure of G172D mature form (Fig. 3) was determined by X-ray crystallography and refined to 1.8 Å resolution with a Rfree of 0.197 and a Rwork of 0.156. Crystallographic data statistics are summarized in Table 1. The mature G172D crystal has two molecules in an asymmetric unit in the triclinic P1 unit cell.

### 3.3. Structural comparison of mature G172D and the wild type GA (2GAW)

To study the effect of Gly to Asp point mutation on the enzyme structure, we compared the mature G172D structure to the wildtype GA structure (2GAW) [7]. Structural comparison revealed that these two structures are essentially identical with an overall rmsd of 0.58 Å for all main chain atom of 536 residues. However, small local shifts of  $\sim 2.3$  Å and 1.7 Å was observed in  $\alpha$ -helices of residues 125–136 and 234–256, respectively. The G172D mutation does not appear to be responsible for these helical shifts since it is more than 8 Å away from the mutation site Asp172. Instead, it is likely to be due to differences in crystal packing of these two structures (P1 vs P21 space groups). Another significant local difference is near the mutation site Asp172 which leads to a 1.3 Å (in molecule A) and 4.1 Å (in molecule B) shift at the main chain between residues Ser 171 to Met 173. Also, at residues Thr 203 and Gly 204 which form the catalytic site, a slight conformational shift of  $\sim 1.3$  Å was observed in G172D structure as compared to the wildtype GA. This shift at the catalytic site was not due to any crystal contact with the neighboring molecules. As a result of the local shift G172D conformation looks very similar to the “closed” conformation observed in the GA-substrate complex [7, 8, 23]

### 3.4. Comparison of wildtype GA-substrate complex with G172D-substrate complex

A time course autoproteolysis assay of G172D mutant in our previous study indicated that it failed to auto-proteolyze to the mature form after incubation at 37°C for 16 hours [17]. However, this mutant did show a very small amount of hydrolase activity when incubated at 37°C for 7 days with the substrate [17]. This very small amount of activity could be due to formation of small amount of mature G172D during the time course experiment. Since now we have the mature G172D crystal structure, we would like to further analyze the effect of Gly to Asp point mutation on hydrolyzing its natural substrate (NAcGlc-Asn). To this end, a G172D-substrate model was generated to compare with the wildtype GA-substrate complex. To model the G172D-substrate complex, the coordinates of substrate (NAcGlc-Asn) from a previously published GA-substrate complex structure (2GL9) [23] were placed into the active site of the current apo-G172D structure by superimposing all secondary structures of GA onto the apo-G172D structure. In this G172D-substrate complex model (Fig. 4), the key residues of GA involved in substrate binding (Trp 11, Thr 152, Arg 180, Asp 183, Thr 203,) interact with the substrate model [23]. The interactions mainly involve hydrogen bonds, salt bridges and van der Waal contacts. Mature G172D-substrate complex showed no drastic change with respect to wildtype GA-substrate complex, except the single amino acid change from Gly to Asp at residue 172, which is located at the edge of the substrate binding pocket (Fig. 4). The bulky aspartic side chain in the G172D mutant is placed near the binding pocket and thus likely affects the binding affinity and substrate processing activity of G172D mutant (see below).

### 3.5. Structural comparison of mature G172D to its precursor form

To study conformational changes after autoproteolysis, G172D mature form was compared to its precursor structure (4R4Y) [17]. In the precursor form of GA, the P-loop (precursor loop) is comprised of 15 residues that connect the  $\alpha$  and  $\beta$  subunits. This loop is released from active site during the enzyme maturation through autoproteolysis. Excluding the P-loop, the overall structure of mature G172D is comparable with the precursor form with an rmsd of 0.72 Å for all main chain atoms of common residues (3–44, 55–136 and 152–295). The slight deviation in rmsd is mainly due to the difference near the P-loop region between the two structures, as a result of releasing the P-loop into bulk solvent after autoproteolysis. In the precursor structure, it has a small cavity near the Asp 172 mutation to accommodate L-aspartic acid  $\beta$  hydroxamate ( $\beta$ -AHA), which acts as an autoproteolysis inhibitor to stabilize the precursor form. After autoproteolysis in the absence of the inhibitor in this study, the G172D mature form adopts a slightly wider conformation at the substrate binding site. There were no other major conformational changes observed between mature G172D and its precursor structure.

### 3.6. Modeling a complex structure between $\beta$ -AHA and wild-type GA

In the previously published precursor G172D- $\beta$ -AHA complex structure [17],  $\beta$ -AHA reversibly binds to the mutant near Asp 172 residue and inhibits the protein autoproteolysis to stabilize the precursor form for structural determination. Binding site of  $\beta$ -AHA in that complex is a partial substrate binding site which involves conserved residues Trp 11, Thr 152, Arg 180, Thr 203 and Gly 204 [7, 23]. As mentioned earlier, GA is capable of

processing a non-chitobiose substrate like  $\beta$ -AHA with its exo-hydrolase activity. However, the detailed catalytic mechanism is not clear. Structural comparisons above among mature G172D mutant, precursor form, and wild type GA suggest that all these proteins have a very similar overall structure with essentially identical conformation near the substrate binding site. This gives us an opportunity to build a wildtype GA- $\beta$ -AHA model based on the structure of the precursor G172D  $\beta$ -AHA complex structure, in order to study the possible mechanism of non-chitobiose substrate processing by wildtype GA. To this end, we built a model complex structure with  $\beta$ -AHA bound in the GA catalytic site, by superimposing multiple GA variants and complexes (see Methods).

Analysis of the wildtype GA-  $\beta$ -AHA complex model (Fig. 5) shows similar interaction of  $\beta$ -AHA and NAcGlc-Asn substrates with the active site residues of GA (Thr 152, Arg 180, Asp 183, Thr 203 and Gly 204). This indicates that interaction of  $\beta$ -AHA with wildtype GA would result in formation of closed conformation similar to enzyme substrate/product complex. However, there is no interaction of  $\beta$ -AHA with the residue Trp 11 which is known to play an important role in binding glycoasparagine substrates [23, 26]. Lack of this interaction may reduce binding affinity of  $\beta$ -AHA when compared to glycoasparagine substrates such as NAcGlc-Asn (see discussions below).

#### 4. Discussion

GA precursor is known to spontaneously autoproteolyze into active mature form after the cleavage of scissile peptide bond between residues Asp151 and Thr 152 [4, 6]. As a result of the autoproteolysis two subunits ( $\alpha$  and  $\beta$ ) are formed. In this study, G172D mutant retained its precursor form after purification and had a negligible hydrolase activity as compared to wild type. The lack in autoproteolytic and hydrolytic activity of this mutant protein could be due to localized conformational changes caused by G172D mutation [17]. However, from our previous study, incubation at 37°C for 7 days did show a small but significant amount of hydrolase activity in G172D mutant [17]. This activity could be due to the presence of very small amount of mature G172D generated after several days of incubation with substrate at 37°C. In our previous study,  $\beta$ -AHA was used to stabilize the precursor G172D structure and we reported a structure of G172D precursor crystal with one of its molecules bound to  $\beta$ -AHA at its defective autoproteolytic site. In the present study, precursor G172D was crystallized without  $\beta$ -AHA and during crystallization it got completely autoproteolyzed into mature form. This suggests that G172D mutant is capable to autoproteolyze slowly into mature form during crystallization. This is consistent with the observation that the current crystal form of mature G172D mutant has the same space group as other GA precursors, but is different from other mature enzymes. Thus, it is likely that precursor G172D became autocleaved into mature form after the protein had initially packed into the crystal as a precursor. When the mature G172D molecule was compared to the wildtype GA, the overall structure of both the molecules were very similar. Also, residues near the active site did not show any drastic change in the conformation. This suggests that mature G172D have similar conformation as wildtype GA near substrate binding site and may acquire closed form upon binding of a substrate leading to its catabolism. Therefore, we modeled a mature G172D-substrate structure and compared it to wildtype GA-substrate complex (Fig. 4). The interaction of catalytic residues of mature G172D to substrate is similar to wildtype. Hence,

mature G172D is likely to acquire a closed conformation upon substrate binding and process with the same mechanism as the wildtype enzyme.

However, G172D-substrate model shows that Asp172 side chain is pointing towards the active site Thr152 (Fig. 6). Interaction of side chain of Asp 172 with both the  $\alpha$ -amino group and the side-chain hydroxyl group of Thr152 could result in polarization of  $\alpha$ -amino group, as well as a compromization on nucleophilicity of the hydroxyl group. Also in the G172D mutant, the linkage between Asp 172 and Met 173 acquired a cis peptide conformation. As a result, the substrate recognition site with residue Arg180 makes a strong interaction with the backbone carbonyl oxygen and nitrogen of Asp 172 and Met 173 respectively. These differential interactions may interfere the substrate binding efficiency of Arg180 in G172D mutant, which may thus lower its overall hydrolase activity when compared to the wildtype GA. Therefore, G172D appears to be able to hydrolyze the substrate but it may not be as efficient as the wildtype GA.

As mentioned above, studies have shown that human GA processes substrate with L-asparagine through its exo-hydrolase activity [15]. From our previous study, it is evident that  $\beta$ -AHA was able to bind to G172D precursor near the substrate binding pocket. The formation of G172D- $\beta$ -AHA complex mimicked wildtype GA structure bound to a substrate in a closed conformation [23]. This leads us to study the mechanism of non-chitobiose substrate processing by GA through the wildtype GA-  $\beta$ -AHA model complex. Residues Thr 152, Arg 180, Thr 203, Gly 204, are known to interact with the L-asparagine portion of the GA hydrolase substrates [8, 23]. Comparison of binding pattern of  $\beta$ -AHA and substrate (NAcGlc-Asn) to wildtype GA shows similar interaction of L asparagine part of both molecules with the conserved residues of GA (Fig 5). Thus GA appears to be capable of processing  $\beta$ -AHA as substrate. In GA, aromatic side chain of Trp 11 has been proposed to facilitate substrate binding via interacting with glycan part of the substrate [23, 26]. However, it has been reported that human GA binds to  $\beta$ -AHA with a  $K_m$  value nine fold higher than its natural substrate NAcGlc-Asn [15]. The higher  $K_m$  value could be explained by the lack of glycan moiety in  $\beta$ -AHA. Analysis of the GA-  $\beta$ -AHA complex model did not reveal any other significant reason for a higher  $k_m$  for  $\beta$ -AHA.

### Catalytic mechanism of non-chitobiose substrate processing by wild type GA

Based on the wildtype GA- $\beta$ -AHA model, we propose a catalytic mechanism by which native GA could process a non-chitobiose substrate (Fig. 7). In this mechanism, free  $\alpha$ -amino group of Thr 152 acts as a base and donates its electrons to the hydroxyl group of Thr 152, making it more nucleophilic in nature. This nucleophilic hydroxyl group of Thr 152 then attacks the carbonyl carbon of  $\beta$ -AHA and forming a covalent bond between enzyme and the substrate. The covalent GA- $\beta$ -AHA transition complex is stabilized by an oxyanion hole, which is likely comprised of the hydroxyl group of Thr 203 and main-chain nitrogen of Gly 204. The negative transition species of GA- $\beta$ -AHA complex is stabilized by making hydrogen-bond interactions with the oxyanion hole through the carbonyl oxygen atom of the transition complex. This complex is later broken by a nearby water molecule (water molecule number 770 in the structure 2GL9 [23]), resulting in release of L-aspartic acid and



a hydroxylamine. Presence of Ser 50 and Thr 170 residues near Thr 152 seems to play a role in catalysis by stabilizing its  $\alpha$ -amino group and nucleophilic hydroxyl group, respectively.

In summary, we reported a high resolution structure of mature form of G172D mutant and studied the effect of its single amino acid change on substrate processing. Based on the mature G172D-substrate model, it is plausible that after autoproteolysis, G172D still be able to hydrolyze substrate although its efficiency could be compromised due to the presence of the bulky Asp 172 side chain in the catalytic cavity. We also analyzed the mechanism by which wild type GA would process  $\beta$ -AHA molecule that lacks a carbohydrate moiety (chitobiose). Similar to other substrates,  $\beta$ -AHA is likely processed through a linked enzyme-L-asparagine intermediate via a Thr152 nucleophilic attack.

## Acknowledgments

We thank Dr. Howard Robinson for assistance on data collection, Lufei Sui and Siavash Mostafavi for assistance on protein purification and enzyme assays. This work was supported by Grant DK075294 from the NIH.

## Abbreviations

<b>AGU</b>	aspartylglucosaminuria
<b>GA</b>	glycosylasparaginase
<b>NAcGlc-Asn</b>	N <sup>4</sup> -( $\beta$ -N-acetylglucosaminyl)-L-asparagine
<b>Ntn</b>	N-terminal nucleophile
<b><math>\beta</math>-AHA</b>	L-aspartic acid $\beta$ -hydroxamate
<b>Asp(pNA)-OH</b>	Aspartic Acid $\beta$ -(p-nitroanilide)
<b>r.m.s.d</b>	root mean square deviation

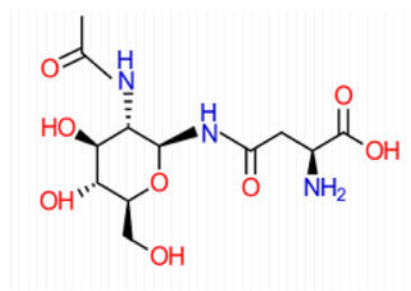
## References

1. Brannigan JA, Dodson G, Duggleby HJ, Moody PC, Smith JL, Tomchick DR, Murzin AG. A protein catalytic framework with an N-terminal nucleophile is capable of self-activation. *Nature*. 1995; 378:416–9. [PubMed: 7477383]
2. Aronson NN Jr, Kuranda MJ. Lysosomal degradation of Asn-linked glycoproteins. *Faseb J*. 1989; 3:2615–22. [PubMed: 2531691]
3. Makino M, Kojima T, Yamashina I. Enzymatic cleavage of glycopeptides. *Biochem Biophys Res Commun*. 1966; 24:961–6. [PubMed: 5970530]
4. Xu Q, Buckley D, Guan C, Guo HC. Structural insights into the mechanism of intramolecular proteolysis. *Cell*. 1999; 98:651–61. [PubMed: 10490104]
5. Wang Y, Guo HC. Crystallographic snapshot of glycosylasparaginase precursor poised for autoprocessing. *J Mol Biol*. 2010; 403:120–130. [PubMed: 20800597]
6. Guan C, Cui T, Rao V, Liao W, Benner J, Lin CL, Comb D. Activation of glycosylasparaginase. Formation of active N-terminal threonine by intramolecular autoproteolysis. *J Biol Chem*. 1996; 271:1732–7. [PubMed: 8576176]
7. Guo HC, Xu Q, Buckley D, Guan C. Crystal structures of *Flavobacterium* glycosylasparaginase: an N-terminal nucleophile hydrolase activated by intramolecular proteolysis. *J Biol Chem*. 1998; 273:20205–20212. [PubMed: 9685368]

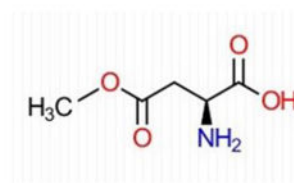
8. Oinonen C, Tikkanen R, Rouvinen J, Peltonen L. Three-dimensional structure of human lysosomal aspartylglucosaminidase. *Nat Struct Biol.* 1995; 2:1102–1108. [PubMed: 8846222]
9. Beaudet, AL., Thomas, GH. Disorders of glycoprotein degradation: mannosidosis, fucosidosis, sialidosis, and aspartylglycosaminuria. In: Scriver, CR, Beaudet, AL, Sly, WS., Valle, D., editors. *The Metabolic Basis of Inherited disease.* Vol. 6. 1989. p. 1603-1622.
10. Kelo E, Dunder U, Mononen L. Massive accumulation of Man2GlcNAc2-Asn in nonneuronal tissue of glycosylasparaginase-deficient mice and its removal by enzyme replacement therapy. *Glycobiology.* 2005; 15:79–85. [PubMed: 15342551]
11. Kartal A, Aydin K. Brain MRI findings in two Turkish Pediatric patients with aspartylglucosaminuria. *Neuroradiol J.* 2016; 5:310–3.
12. Kaartinen V, Mononen I, Voncken JW, Noronkoski T, Gonzalez-Gomez I, Heisterkamp N, Groffen J. A mouse model for the human lysosomal disease aspartylglycosaminuria. *Nat Med.* 1996; 2:1375–8. [PubMed: 8946839]
13. Noronkoski T, Stoineva IB, Petkov DD, Mononen I. Recombinant human glycosylasparaginase catalyzes hydrolysis of L-asparagine. *FEBS Lett.* 1997; 412:149–52. [PubMed: 9257709]
14. Noronkoski T, Stoineva IB, Ivanov IP, Petkov DD, Mononen I. Glycosylasparaginase-catalyzed synthesis and hydrolysis of beta-aspartyl peptides. *J Biol Chem.* 1998; 273:26295–7. [PubMed: 9756857]
15. Kaartinen V, Mononen T, Laatikainen R, Mononen I. Substrate specificity and reaction mechanism of human glycoasparaginase. The N-glycosidic linkage of various glycoasparagines is cleaved through a reaction mechanism similar to L-asparaginase. *J Biol Chem.* 1992; 267:6855–8. [PubMed: 1551892]
16. Coulter-Mackie MB. A novel exonic mutation in the aspartylglucosaminidase gene causes exon skipping. *J Inherit Metab Dis.* 1999; 22:682–683. [PubMed: 10399108]
17. Sui L, Lakshminarasimhan D, Pande S, Guo HC. Structural basis of a point mutation that causes the genetic disease aspartylglucosaminuria. *Structure.* 2014; 22:1855–61. [PubMed: 25456816]
18. Gordon BA, Rupa CA, Rip JW, Haust MD, Coulter-Mackie MB, Scott E, Hinton GG. Aspartylglucosaminuria in a Canadian family. *Clin Invest Med.* 1998; 21:114–123. [PubMed: 9627765]
19. Cui T, Liao PH, Guan C, Guo HC. Purification and crystallization of precursors and autoprocessed enzymes of *Flavobacterium glycosylasparaginase*: an N-terminal nucleophile hydrolase. *Acta Crystallogr D Biol Crystallogr.* 1999; 55:1961–4. [PubMed: 10531509]
20. The CCP4 suite: programs for protein crystallography. *Acta Crystallogr D Biol Crystallogr.* 1994; 50:760–3. [PubMed: 15299374]
21. Qian X, Guan C, Guo HC. A dual role for an aspartic acid in glycosylasparaginase autoproteolysis. *Structure.* 2003; 11:997–1003. [PubMed: 12906830]
22. Emsley P, Cowtan K. Coot: model-building tools for molecular graphics. *Acta Crystallogr D Biol Crystallogr.* 2004; 60:2126–32. [PubMed: 15572765]
23. Wang Y, Guo HC. Crystallographic snapshot of a productive glycosylasparaginase-substrate complex. *J Mol Biol.* 2007; 366:82–92. [PubMed: 17157318]
24. Heiskanen T, Tollersrud OK, Zhao M, Peltonen L. Large-scale purification of human aspartylglucosaminidase: utilization of exceptional sodium dodecyl sulfate resistance. *Protein Expr Purif.* 1994; 5:205–210. [PubMed: 8054856]
25. Wang Y, Guo HC. Two-step dimerization for autoproteolysis to activate glycosylasparaginase. *J Biol Chem.* 2003; 278:3210–3219. [PubMed: 12433919]
26. Liu Y, Guan C, Aronson NN Jr. Site-directed mutagenesis of essential residues involved in the mechanism of bacterial glycosylasparaginase. *J Biol Chem.* 1998; 273:9688–9694. [PubMed: 9545303]

### Highlights

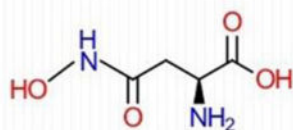
- Precursor of a Canadian-AGU mutant autoproteolyzes to mature form after crystallization
- Effect of a Gly to Asp mutation on hydrolytic activity of GA enzyme
- Proposed mechanism for non-chitobiose substrate processing by wildtype GA



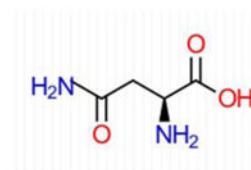
N<sup>4</sup>-(β-N-acetylglucosaminy)-L-asparagine  
(NAcGlc-Asn)



L-aspartic acid β-methyl ester

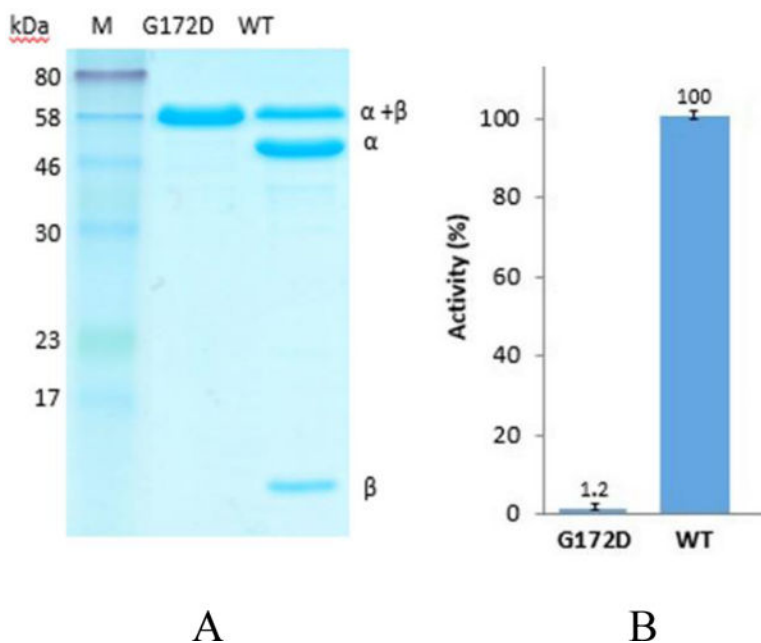


L-aspartic acid β-hydroxamate  
(β-AHA)



L- asparagine

**Fig. 1.** Chemical structures of representative GA substrates, including glycoasparagines, non-chitobiose β-AHA, and L-asparagine.

**Fig 2.**

Autoproteolytic and hydrolase activity of G172D mutant with respect to the wild type GA. (A) SDS-PAGE analysis of G172D and wildtype proteins, which were expressed and purified as MBP-tagged proteins. We have previously demonstrated that the N-terminal MBP-tag (42 kDa) does not alter GA structure or function [19, 25]. For an untagged *Flavobacterium* GA, the precursor form is 32kDa, which is then autocleaved into alpha (17 kDa) and beta (15 kDa) subunits. In this figure, the bands with molecular weight ~74 kDa represent MBP+precursor form. The molecular weight of autoproteolyzed MBP+ alpha subunit is 58 kDa, and beta subunit is 15 kDa. WT is the wild type GA. Lane M represents marker bands. (B) Hydrolysis activity. The activity of wild type GA is normalized to 100%. Data are average of three repeats with standard error shown as an error bar.

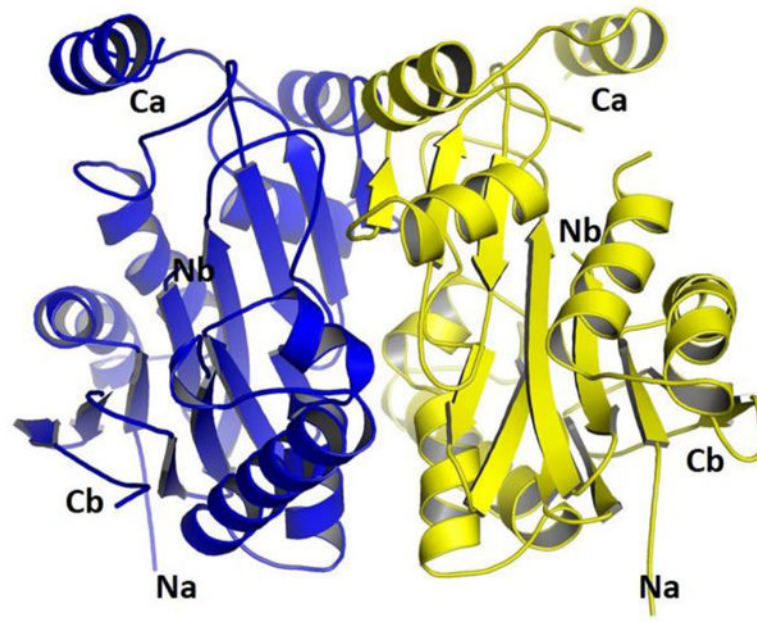


**Fig 3.** Overall structure of mature G172D crystal. The structure consists of two molecules in a GA biomolecular assembly (one in blue and the other in yellow color) with one alpha and one beta chain in each molecule. Ca and Cb represent carboxyl termini of alpha and beta subunits, respectively, in each molecule. Na and Nb represent amino termini of alpha and beta subunits, respectively, in each molecule.

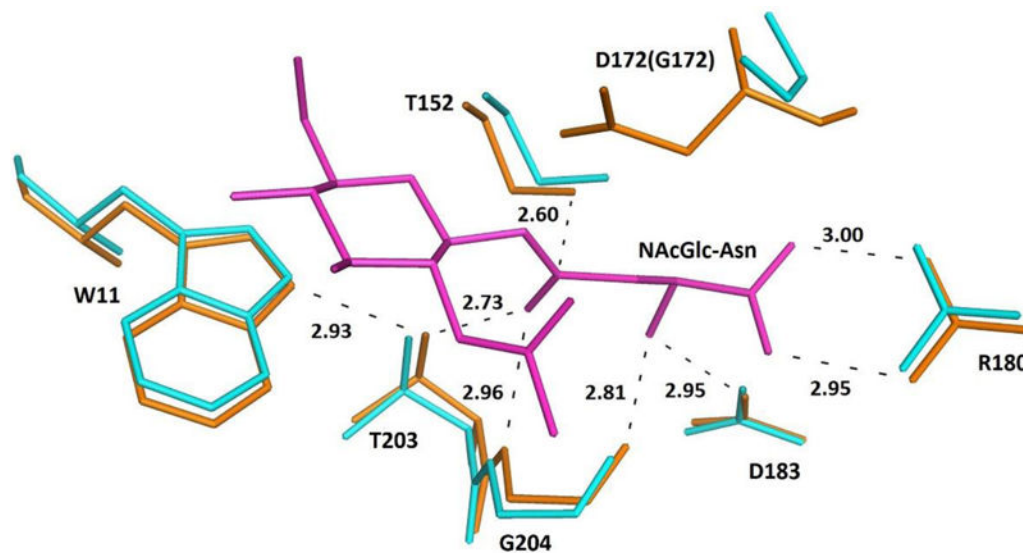


**Fig. 4.** Detailed interactions of NAcGlc-Asn substrate (in pink) with mature G172D (in brown color). Corresponding residues of wildtype GA are also shown for reference in cyan color. The dotted lines denote the hydrogen bond interactions (with the distance in Å) between substrate and G172D at the substrate binding pocket.

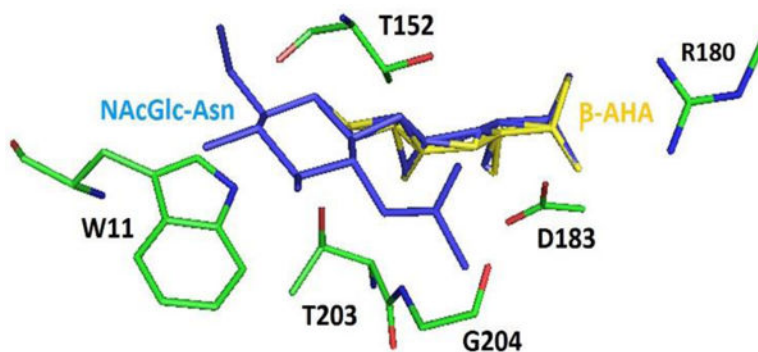


**Fig. 5.** Complex model illustrating binding of  $\beta$ -AHA and (NAGlc-Asn) as substrates of wild-type GA.  $\beta$ -AHA is shown in yellow and (NAGlc-Asn) substrate in blue color. Selective residues of GA forming the substrate binding site are shown in green.



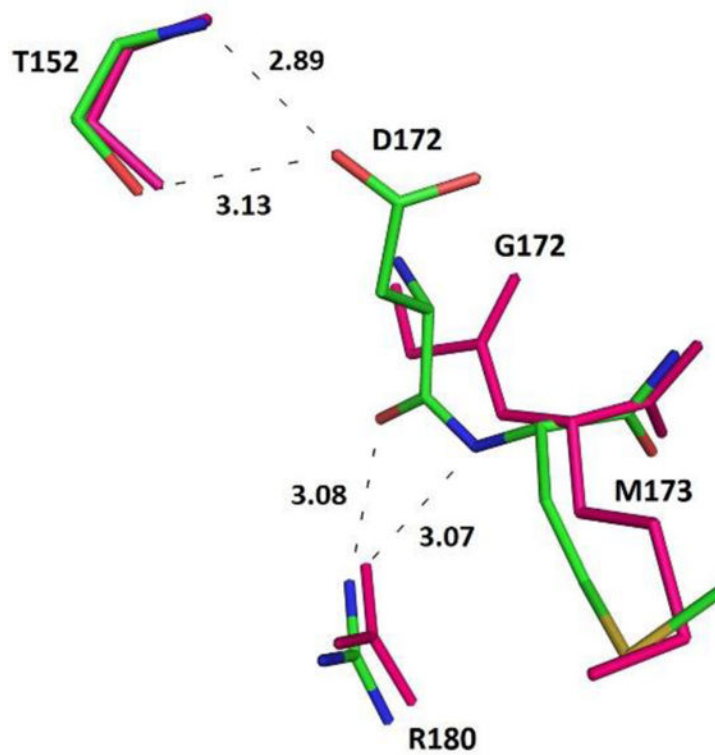


**Fig. 6.** Differential interactions as a result of the mutation at residue 172, a change from G172 to D172. Selective residues in pink represent wildtype GA while the ones in green are mature G172D mutant. The dotted lines denote the hydrogen bond interactions (with the distance in Å) among G172D active site residues.

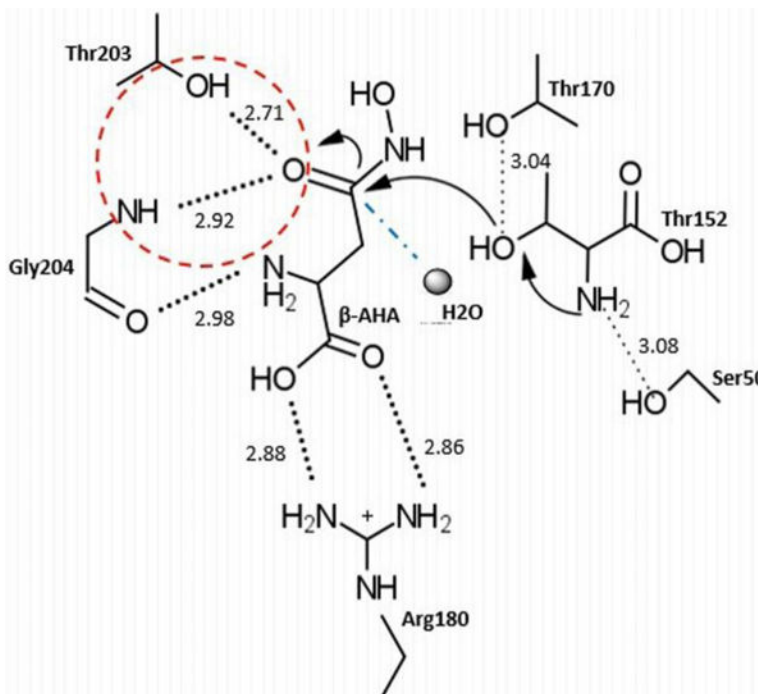


**Fig. 7.** Mechanistic model of  $\beta$ -AHA catalysis by wildtype GA. The proposed catalytic reaction mechanism of a non-chitobiose substrate ( $\beta$ -AHA) processing by wild type (mature form) via Thr152 nucleophilic attack and oxanion hole formation. Dashed lines represent hydrogen bond interactions with distances designated in angstroms. Large dotted circle represents oxanion hole, and small grey circle represents a water molecule. The curved arrows indicate nucleophilic attack and routes of leaving groups.

**Table 1**

## Crystallographic Data Collection and Refinement Statistics

<b>G172D Mature Form Crystal</b>	
Resolution (Å) <sup>a</sup>	50.1–1.83 (1.87–1.83)
Space Group	P1
Cell Dimensions:	
a, b, c (Å)	46.0 52.8 61.9
α, β, γ (°)	81.5 90.2 105.9
No. of molecules per asymmetric unit	2
I/σ-I	18.8 (9.7)
Completeness (%)	92.6 (92.3)
<i>R</i> <sub>sym</sub> (%) <sup>b</sup>	4.4 (9.6)
Structure refinement	
Resolution (Å)	20–1.83
No. of reflections	42,925 (2,435)
<i>R</i> <sub>work</sub> <sup>c</sup>	0.156
<i>R</i> <sub>free</sub> <sup>d</sup>	0.197
R.m.s. deviations <sup>e</sup>	
Bond-lengths (Å)	0.02
Bond-angles (°)	1.9
Ramachandran plot	
Most favored regions (%)	97.2
Additional allowed regions (%)	2.4
Outliners (%)	0.4
B-factors (Å <sup>2</sup> )	
Main chain	15.6
Side chain	20.1
Water	25.4

<sup>a</sup>Numbers in parenthesis refer to the outermost resolution bin.

<sup>b</sup> $R_{sym} = \frac{\sum_i \sum_j |I_{hi} - I_{hj}|}{\sum_i \sum_j I_{hi}}$  for the intensity (*I*) of *i* observation of reflection *h*.

<sup>c</sup> $R_{work} = \frac{\sum |F_{obs} - F_{calc}|}{\sum |F_{obs}|}$ , where *F*<sub>obs</sub> and *F*<sub>calc</sub> are the observed and calculated structure factor amplitudes, respectively.

<sup>d</sup>*R*<sub>free</sub> was calculated as *R*<sub>work</sub>, but with 5% of the amplitudes chosen randomly and omitted from the start of refinement.

<sup>e</sup>R.m.s. deviations are deviations from ideal geometry.